https://doi.org/10.22226/2410-3535-2023-3-272-277

Quasi-static crack growth in three-layer media: a numerical experiment

R. L. Lapin[1], V. A. Kuzkin[†,1,2], A. M. Krivtsov[1,2]

[†]kuzkinva@gmail.com

[1]Peter the Great Saint Petersburg Polytechnic University, St. Petersburg, 195251, Russia
[2]Institute for Problems in Mechanical Engineering RAS, St. Petersburg, 199178, Russia

Quasi-static growth of planar three-dimensional cracks in homogeneous and three-layer media is studied numerically using the particle dynamics method. It is shown that in the homogeneous medium cracks with different convex and nonconvex initial shapes tend to become circular (penny-shaped). The crack "forgets" its initial chape approximately when its front reaches the corresponding circumscribed circle and further propagates in the penny-shaped mode. In the three-layer medium, a crack grows in the plane orthogonal to the layers, having either different Young's moduli or different strength. In simulations, the ratio of crack's length (size along the layers) to its height (size across the layers) is calculated. It is shown that with increasing crack volume the ratio tends to some limiting value, dete272rmined by contrast in properties of the layers. Empirical dependencies of the limiting length/height ratio on parameters of the layers are derived. The conditions, corresponding to arresting of the crack in the central layer, are estimated.

Keywords: crack, quasi-static growth, layered medium, particle dynamics method, crack shape.

1. Introduction

Modelling of propagation of cracks in layered materials is a classical problem in mechanics of solids having various practical applications. The practical significance of this problem is due to the fact that many natural and human-made materials have a layered structure, i. e. consist of interconnected layers with different mechanical properties. The list of layered materials includes, but is not limited to, rocks, plants, biomaterials, composites, coatings etc.

Mismatch of mechanical properties of the layers significantly influences the propagation of cracks. In layered materials, three main scenarios of crack growth are possible, namely, (i) propagation of a crack in one material parallel to the layers, (ii) propagation of a crack along the interface between layers (delamination, see e. g. the review [1]), and (iii) propagation at some angle to the layers. In the present paper, we focus on the third scenario, when the crack propagates perpendicular to the layers. Transition from normal propagation to delamination is not observed in our numerical simulations. We refer e. g. to papers [2, 3] for analysis of this transition and corresponding criteria.

In some cases, crack propagation is not desired, while in the others it is the main goal of the technological process. One example of crack propagation normal to layers is hydraulic fracturing [4–8]. In hydraulic fracturing, a vertical crack propagates in the layered rock under the action of a viscous fluid or a mixture, pumped into the crack at high pressure. Since oil-containing layers are often surrounded by water-containing layers, accurate prediction of the crack shape is of key importance for successful and efficient hydraulic fracturing. Therefore, mathematical models describing propagation of cracks in layered media are required.

Investigation of crack propagation in layered materials is challenging from both experimental and theoretical points of view. Real experiments are usually expensive and complicated or even impossible as in the case of full-scale hydraulic fracturing. Therefore, the amount of available experimental data on propagation of cracks in layered materials is limited. In this case, "numerical experiments", i. e. direct numerical simulation of crack propagation in layered media, may serve as a source of information for development of analytical or semi-analytical models, needed in engineering applications.

In literature, propagation of cracks in brittle inhomogeneous media is mostly simulated in the framework of linear fracture mechanics. Fracture criteria based on the stress intensity factor are often used. Despite the well-developed apparatus of computational linear fracture mechanics, modeling of propagation of three-dimensional cracks in layered materials is not straightforward for several reasons. In the framework of finite element method, fine mesh in the vicinity of crack front and remeshing are required, while boundary element method requires calculation of the Green's function for the layered medium [9,10,11]. Additionally, the stress intensity factor and therefore classical fracture criteria loose sense, when the crack tip is located at the interface between layers [12]. To avoid these difficulties, we use the particle dynamics method (see e. g. [13]) for simulation of crack propagation. In the framework of the particle dynamics, the material is represented by a set of interacting particles (material points or rigid bodies). The particles are connected by springs, which break when their deformation reaches some critical value. The set of broken springs can be interpreted as a crack. To simulate quasi-static processes, viscous forces acting on the particles are also introduced. Equations of motion for the particles are solved numerically

using explicit methods. Main advantages of the particle dynamics are relatively simple computer implementation and clear physical meaning of model parameters. Therefore, particle dynamics method and other particle-based methods (e. g. the discrete element method [14]) are widely used for simulation of brittle fracture [15–17].

In the present paper, we use the particle dynamics method for numerical experiments on propagation of cracks in three-layer media with layers having either different Young's moduli or different strength. Using the results of numerical experiments, we propose simple empirical formulae, describing dependence of the length/height ratio of the crack on contrast in parameters of the layers.

2. Discrete model of the layered medium

In this section, we describe the model of a brittle, three-layer material, based on the particle dynamics method. A cube of a material is considered under periodic boundary conditions. The material is represented as a set of interacting particles. To create layers with isotropic mechanical properties, the algorithm for generation of the quasi-random lattice is used [18]. The algorithm works as follows. Firstly, the particles are placed at positions of nodes of the ideal face-centered cubic (FCC) lattice with a lattice constant d (see Fig. 1). Secondly, to break the symmetry (and corresponding anisotropy) of the FCC lattice, each particle is randomly displaced. The resulting configuration is shown in Fig. 1. Each pair of particles with distance of less than $1.9d$ is connected by an undeformed linear spring. In paper [18], it is shown that the resulting material is elastically isotropic.

Dynamics of the particles is governed by the equations of motion

$$m\dot{\mathbf{v}}_i = \sum_j \mathbf{F}_{ij} - \gamma \mathbf{v}_i, \tag{2.1}$$

where $\mathbf{v}_i$ is velocity of the particle i, m is the particle mass, $\mathbf{F}_{ij}$ is the force in the spring connecting particles i and j, γ is the damping constant. In formula (2.1), summation is carried out over all particles j connected to the particle i. The force $\mathbf{F}_{ij}$ is determined by the formula

$$\mathbf{F}_{ij} = c_{ij}\left(d_{ij} - d_{ij}^0\right)\mathbf{e}_{ij},\ d_{ij} - d_{ij}^0 \le \varepsilon_c d_{ij}^0,\ c_{ij} = cd / d_{ij}^0, \tag{2.2}$$

where c_{ij} is the stiffness of the spring, d_{ij}^0, d_{ij} are the initial and the current distances between the particles, $\mathbf{e}_{ij}$ is the unit vector directed along the line, connecting particles i and j, ε_c is the critical deformation, corresponding to breakage of the bond, and c is the parameter, determining stiffness of the material. If deformation of the spring, connecting particles i and j, exceeds the critical value (i. e. if $d_{ij} - d_{ij}^0 > \varepsilon_c d_{ij}^0$) then the stiffness c_{ij} is set to zero and the additional force F_p is applied to particles i, j to simulate the internal pressure in the crack. The magnitude of the force is calculated as

$$F_p = \begin{cases} \dfrac{Ac_0 d^4 t}{\left(d^3 + V(t)\right)\tau_*}, & V(t) \le d^3, \\ \dfrac{Ac_0 d^4 t}{V(t)\tau_*}, & V(t) > d^3, \end{cases} \tag{2.3}$$

where $A = 10^{-3}$, $\tau_* = 2\pi\sqrt{m/c_0}$, the crack volume $V(t)$ is defined as the sum of elongations of all springs associated with the crack, multiplied by the average area per spring. The forces (2.3) form spatially uniform pressure in the crack. Inverse proportionality of the pressure on the crack volume is used in order to avoid unstable crack growth.

To set different properties of the three layers in the cubic specimen, we use the following dependence of parameters c, ε_c on y coordinate (the crack propagates in the xy-plane):

$$c = \begin{cases} c_0, & \left|\dfrac{y}{w}\right| \le \dfrac{1}{12} \\ \dfrac{E_1}{E_0} c_0, & \left|\dfrac{y}{w}\right| > \dfrac{1}{12} \end{cases}, \qquad \varepsilon_c = \begin{cases} \varepsilon_0, & \left|\dfrac{y}{w}\right| \le \dfrac{1}{12} \\ \dfrac{\sigma_c^1}{\sigma_c^0}\varepsilon_0, & \left|\dfrac{y}{w}\right| > \dfrac{1}{12} \end{cases}. \tag{2.4}$$

Here w is size of the cubic specimen, parameters E_1/E_0 and σ_c^1/σ_c^0 are ratios of Young's muduli and uniaxial tensile strength of the layers. Macroscopic mechanical properties of the central layer are related to c_0, ε_0 by the empirical formulae obtained in paper [18]:

$$\nu \approx 0.255,\quad E_0 \approx 1.48 c_0/d,\quad \sigma_c / E_0 \approx 4.1\varepsilon_0, \tag{2.5}$$

where ν is Poisson's ratio. These formulae can be used to calculate the properties of the bounding layers, provided that spring stiffness and critical deformation, given by (2.4) are used.

The equations of motion (2.1)–(2.4) with zero initial conditions are solved numerically using symplectic leap-frog integration scheme with time step $\Delta t = 0.003\tau_*$, where $\tau_* = 2\pi\sqrt{m/c_0}$. Evolution of the crack, formed by a set of broken (zero-stiffness) springs, with increasing crack volume is investigated.

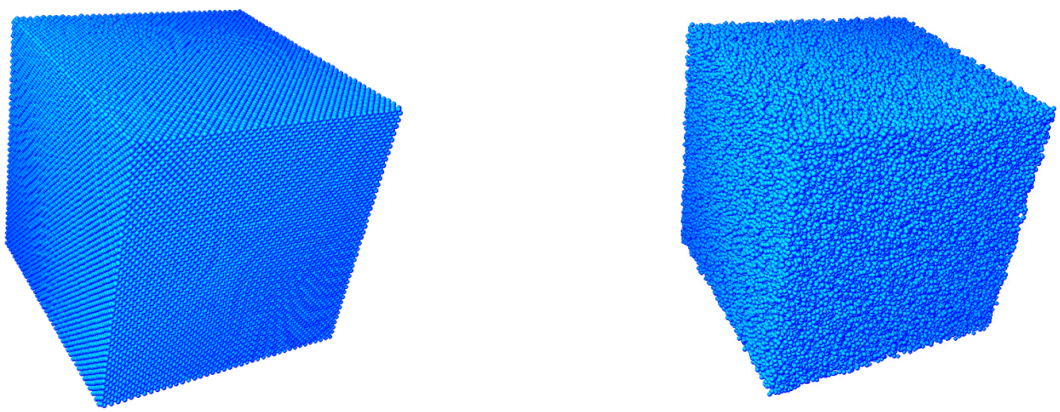

Fig. 1. Face-centered cubic lattice (left) and a quasi-random lattice (right).

3. Crack in a homogeneous medium

In this section, we investigate evolution of flat cracks of different initial shapes. The cracks grow in macroscopically homogeneous material ($E_1/E_0=1$, $\sigma_c^1/\sigma_c^0=1$ in formula (2.4)). Rectangular, triangular, and star-like initial crack shapes are considered. To create the initial crack, at $t=0$ springs intersecting the corresponding flat geometric shape (rectangle, triangle or star) are found. Stiffness of the springs is set to zero and the force F_p, defined by (2.3), is applied to particles connected by these springs. Simulations are carried out with the following values of parameters:

$$w=100d, \quad \frac{E_1}{E_0}=1, \quad \frac{\sigma_c^1}{\sigma_c^0}=1, \quad \varepsilon_0=2\cdot 10^{-5},$$
$$\Delta t=0.003\tau_*, \quad N\approx 10^5,$$
$$\tau_*=2\pi\sqrt{m/c_0}, \quad \gamma=2\sqrt{mc_0},$$

where Δt is the time step, N is the number of particles. During the simulation, the crack front is determined using the set of all springs with zero stiffness. For visualization of convex cracks, their front is approximated by polygons using the algorithm described in paper [19] (see Fig. 2). Non-convex cracks are visualized by showing springs with zero stiffness (see Fig. 3).

Evolution of initially rectangular and triangular cracks is shown in Fig. 2. Different lines correspond to crack fronts calculated at regular time intervals equal to $300\tau_*$. The initial cracks are shown by black lines.

It is seen from Fig. 2 that for both initial crack shapes, the cracks become nearly circular (penny-shaped) approximately when their fronts reach the corresponding circumscribed circles. Further the crack shape does not change due to symmetry of the problem. Deviations from the circular shape are due to microscopic inhomogeneity of the discrete material model. Therefore, the crack "forgets" its initial shape.

In the case of a more complex, non-convex initial crack shape, the results are similar. For example, growth of an initial star-like crack is shown in Fig. 3. It is seen that the crack starts to grow from the inner angles of the star. This fact is consistent with results of paper [20], where it is shown that the stress intensity factor for the star-like crack has maxima in the inner angles of the star. The crack rapidly become nearly circular.

Thus, our simulation results show that an arbitrary planar crack, growing in a homogeneous medium under the uniform internal pressure, tends to become penny-shaped. This fact is consistent with numerical results (see e.g. the review [21]) and qualitative estimates [22] obtained in the framework of continuum linear fracture mechanics. We note that similar phenomenon of vanishing influence of initial conditions on propagation of cracks is also observed in simulations of hydraulic fracturing, where propagation of a crack under the action of constantly pumped fluid is considered [8].

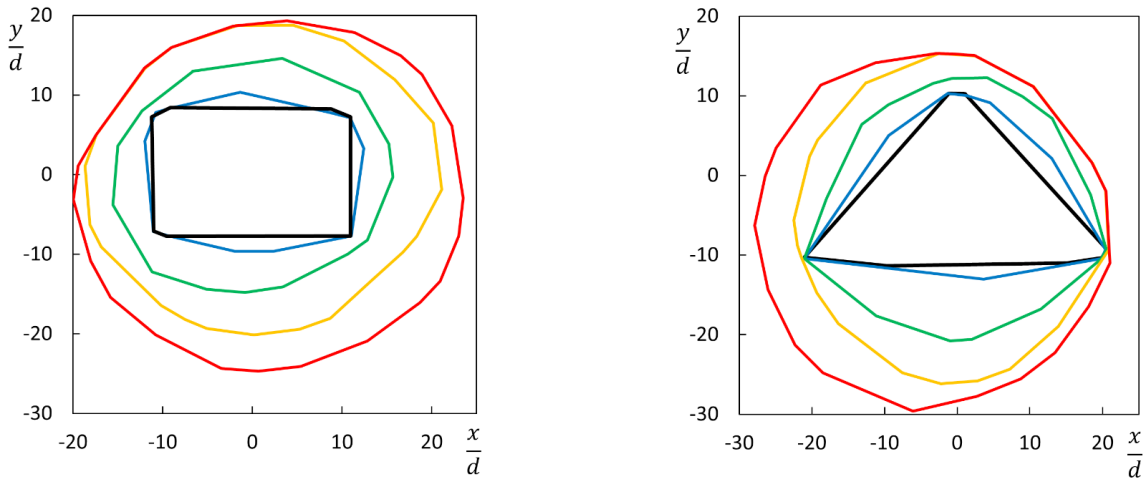

Fig. 2. (Color online) Quasi-static growth of cracks in a macroscopically homogeneous medium. Initial cracks are shown by thick black lines. Colored lines correspond to crack fronts, calculated at regular time intervals equal to $300\tau_*$.

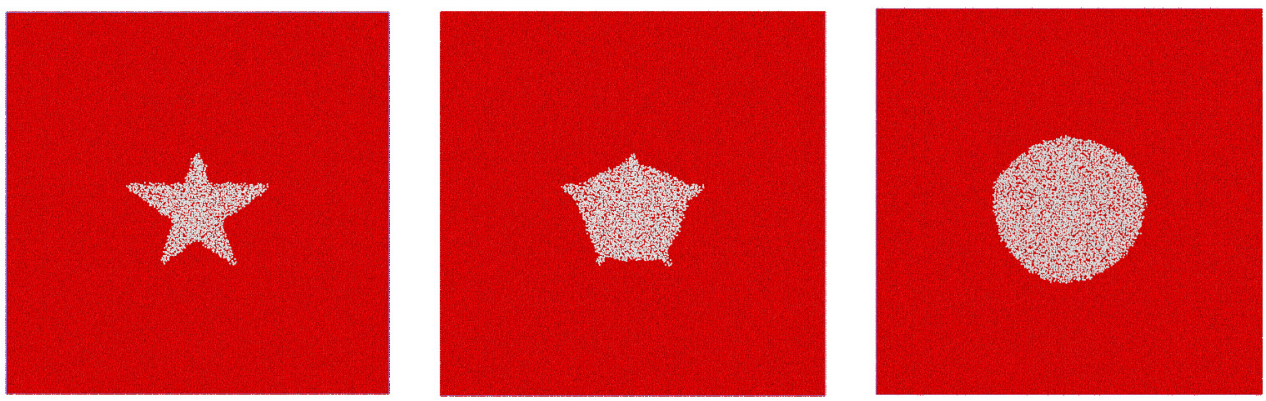

Fig. 3. (Color online) Quasi-static growth of a star-like crack in a macroscopically homogeneous medium. Particles with broken (zero-stiffness) bonds, forming the crack, at different times are shown by white color.

4. Crack propagation in a three-layer medium

In this section, quasi-static crack growth in a three-layer medium is considered (see Fig. 4). It is assumed that the upper and lower layers have the same properties (equal c and ε_c, see (2.4)), different from the properties of the central layer (see formula (2.4)). In what follows, the upper and lower layers are referred to as the bounding layers. The influence of contrast in Young's moduli and strengths of the layers on the evolution of the crack shape is considered. In simulations, the following values of parameters are used

$$w=160d,\ R=0.15w,\ \varepsilon_0=2\cdot10^{-5},\ \Delta t=0.003\tau_*,\ N=10^7, \quad (4.1)$$

where R is the radius of the initial crack.

The main parameter calculated in the simulations is the length/height ratio of the crack. The crack length L is defined as the maximal crack size along the layers, while the crack height H is defined as the maximal crack size in the direction across the layers. Calculating this parameter, we answer the question of whether the crack mostly grows along the central layer or into the bounding layers. We also estimate the conditions corresponding to arresting of the crack in the central layer.

4.1. Layers with different Young's moduli

In this subsection, we study the influence of the contrast in Young's modulus of the layers on the crack shape. Bounding layers have the same Young's modulus E_1, while the central layer has different Young's modulus E_0. We consider influence of the parameter E_1/E_0 in formula (2.4) on the crack shape (the L/H ratio).

The dependence of the L/H ratio on the crack volume at various contrasts in Young's modulus is presented in Fig. 5. It is seen that if the central layer is stiffer than the bounding layers (i. e. $E_0>E_1$) then the crack grows mostly in the central layer. For E_1/E_0 less than approximately 0.25 the crack remains locked in the central layer. In this case, L/H tends to infinity with increasing crack volume, while H is equal to the width of the central layer. In contrast, if the central layer is softer than the bounding layers ($E_0<E_1$) then the crack grows mostly into the bounding layers.

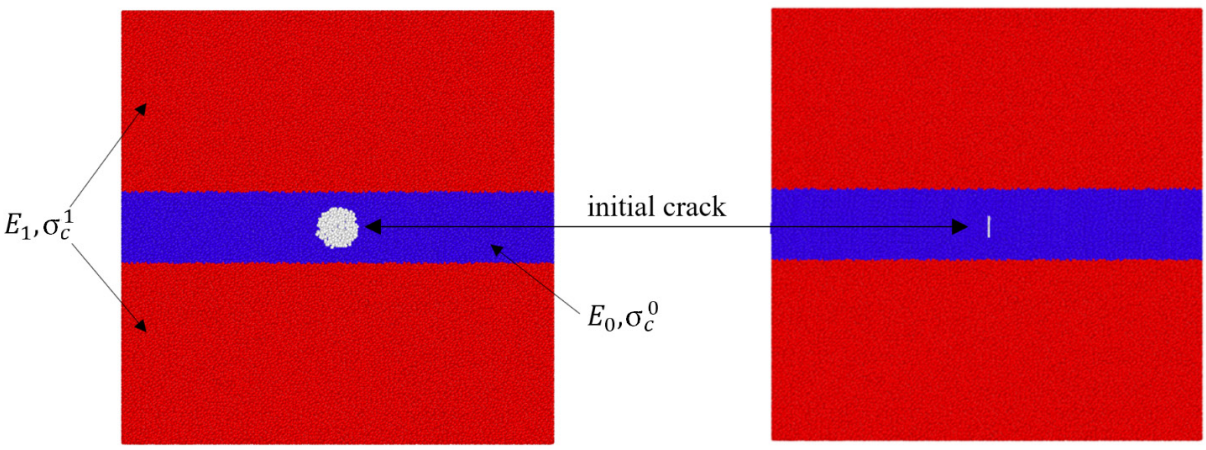

Fig. 4. (Color online) Initial crack in a three-layered medium: front view (left) and top view (right). Particles with zero-stiffness bonds, forming the crack, are shown in white.

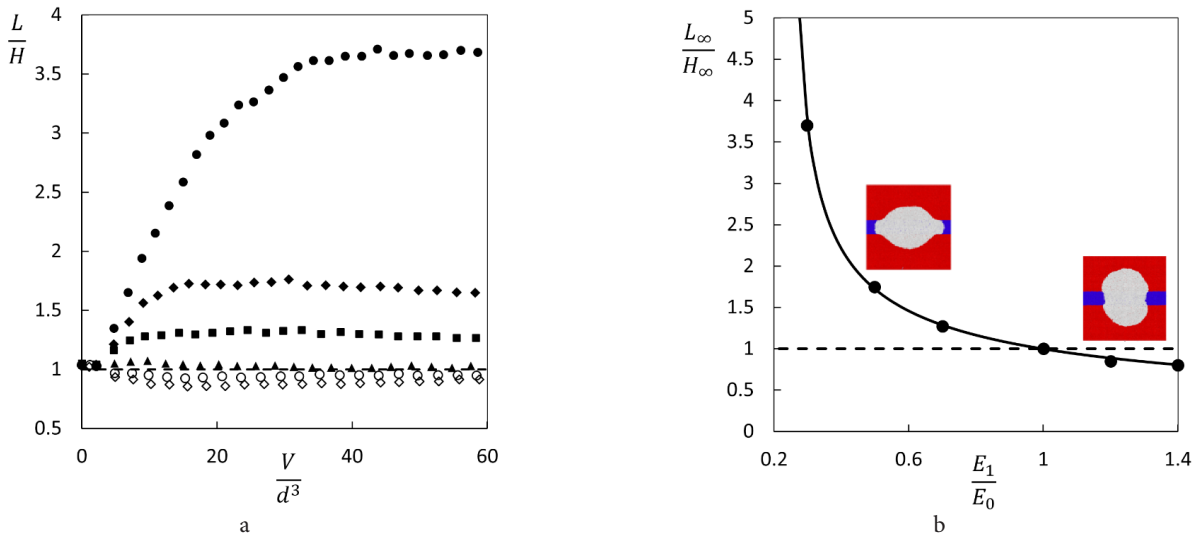

Fig. 5. (Color online) The dependence of the L/H ratio on the crack volume V at various ratios of elastic moduli E_1/E_0. Results for E_1/E_0 equal to 0.3 (circles), 0.5 (diamonds), 0.7 (squares), 1 (triangles), 1.2 (empty circles), and 1.4 (empty diamonds) are shown (a). Limiting value of the length/height ratio (L_∞/H_∞) at large volumes for different values of E_1/E_0. Numerical results (dots) and approximation by the formula (4.2) (solid line) are shown. The inner figures show crack shapes for E_1/E_0 equal to 0.5 (left) and 1.2 (right) (b).

For $E_1/E_0 > 0.25$, the L/H ratio tends to some asymptotic value with increasing crack volume. To find this asymptotic value, for each value of E_1/E_0 several simulations with different initial distributions of particles in the material are performed. The results presented in Fig. 5 correspond to averaging over 5 simulations. The numerical results are approximated by the following empirical formula

$$\frac{L_\infty}{H_\infty} = \lim_{V\to\infty}\frac{L}{H} \approx \sqrt{\frac{1-\alpha_*}{E_1/E_0-\alpha_*}}, \qquad (4.2)$$

where α_* is the critical ratio of moduli, corresponding to arresting of the crack in the central layer. Fitting of the numerical data yields $\alpha_* \approx 0.245$.

Thus, simulation results show that crack tends to grow into the stiffer layer. This result is in a qualitative agreement with the results obtained by entirely different means in paper [5], where influence of elastic modulus mismatch on propagation of hydraulic fractures is investigated.

4.2. Layers with different strength

In this subsection, we discuss crack propagation in a specimen, consisting of three layers with different strength. Strength of the bounding layers is equal to σ_c^1, while strength of the central layer is equal to σ_c^0. Elastic properties of all layers are the same. We consider influence of the parameter σ_c^1/σ_c^0 in formula (2.4) on the crack shape (the L/H ratio). Values of σ_c^1/σ_c^0 in the interval from 0.6 to 1.6 are considered. For larger σ_c^1/σ_c^0, size of the computational domain given by (4.1) is not sufficient.

The dependence of the L/H ratio on the crack volume V at various strength ratios σ_c^1/σ_c^0 is presented in Fig. 6. If the central layer has larger strength ($\sigma_c^0 > \sigma_c^1$) then the crack tends to grow mostly in the bounding layers. With increasing volume, the L/H ratio tends to some constant value less then 1. If the bounding layers have larger strength than the central layer ($\sigma_c^0 < \sigma_c^1$) then the crack mostly grows along the central layer. With increasing crack volume, the L/H ratio either tends to some limiting value (for σ_c^1/σ_c^0 approximately less than 2) or tends to infinity for larger σ_c^1/σ_c^0. In other words, the crack remains arrested (locked) in the central layer, if the bounding layers are approximately twice stronger than the central layer.

For σ_c^1/σ_c^0 in the interval [0.6; 1.6], the L/H ratio tends to the limiting value L_∞/H_∞ as the crack volume increases. To find the limiting value L_∞/H_∞ several calculations are performed with different initial configurations of particles. The resulting L_∞/H_∞ averaged over 5 realizations are presented in the Fig. 6b. These results are approximated by the empirical formula

$$\frac{L_\infty}{H_\infty} \approx \frac{1-\beta_*}{\sigma_c^1/\sigma_c^0-\beta_*}, \qquad (4.3)$$

where β_* is the critical strength ratio, corresponding to arresting of the crack in the central layer. Fitting of the numerical data yields $\beta_* \approx 1.85$. We note that since the exact type of dependence of L_∞/H_∞ on σ_c^1/σ_c^0 is unknown then this value of β_* should be considered as a rough estimate.

5. Conclusions

We have presented results of numerical experiments on quasi-static propagation of cracks in homogeneous and three-layer media under the action of uniform internal pressure. Evolution of the crack shape with increasing crack volume was investigated.

In the homogeneous medium, a crack of an arbitrary initial shape tends to become penny-shaped. The diameter of the penny-shaped crack is of order of the maximum size of the initial crack. These results are consistent with the prediction of continuum linear fracture mechanics [21,22].

In the three-layer media, the crack shape is determined by contrast in parameters of the layers. The influence of the contrast in elastic moduli and strength of the layers was considered. Length/height ratio of the crack as a function of the crack volume was calculated. It was shown that the ratio

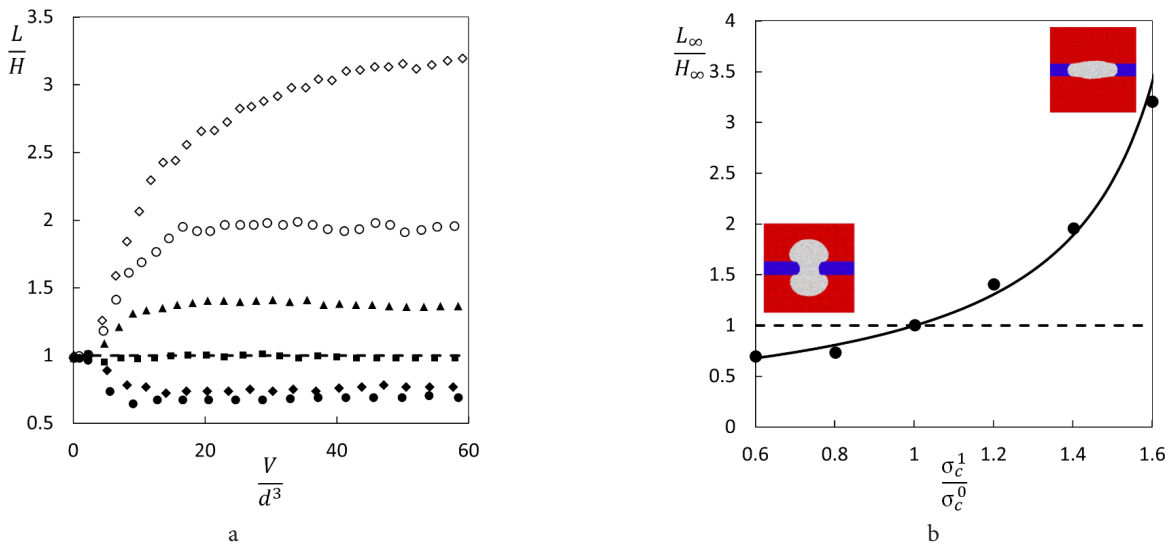

Fig. 6. (Color online) The dependence of the L/H ratio on the crack volume V at various strength ratios σ_c^1/σ_c^0. Results for σ_c^1/σ_c^0 equal to 0.6 (circles), 0.8 (diamonds), 1 (squares), 1.2 (triangles), 1.4 (empty circles), and 1.6 (empty diamonds) are shown (a). Limiting value of the length/height ratio (L_∞/H_∞) at large volumes for different strength ratios σ_c^1/σ_c^0. Numerical results (dots) and approximation by formula (4.5) (solid line) are shown. The inner figures show crack shapes for σ_c^1/σ_c^0 equal to 0.6 (left) and 1.6 (right) (b).

tends to some limiting value as the crack volume increases. The limiting length/height ratio decreases with increasing Youngs' modulus of the bounding layers, while it increases with increasing strength of the bounding layers. Conditions, corresponding to arresting of the crack in the central layer were determined. The crack remains in the central layer if either the central layer is approximately four times stiffer or twice weaker than the bounding layers. Simple empirical formulae relating the limiting length/height ratio with contrast in properties were proposed.

Acknowledgments. The authors are deeply grateful to A. B. Freidin and M. L. Kachanov for stimulating discussions. A. M. K.'s work was supported by the Russian Science Foundation, grant no. 21-11-00378.

References

1. M. Comninou. Eng. Fract. Mech. 37 (1), 197 (1990).
2. M.-Y. He, J. W. Hutchinson. Int. J. Sol. Struct. 25 (9), 1053 (1989). Crossref
3. T. Siegmund, N. A. Fleck, A. Needleman. Int. J. Fract. 85 (4), 381 (1997). Crossref
4. M. M. Khasanov, G. V. Paderin, E. V. Shel, A. A. Yakovlev, A. A. Pustovskikh. Neftyanoe khozyaystvo-Oil Industry. 12, 37 (2017). Crossref
5. H. Gu, E. Siebrits. SPE Production & Operations. 23 (02), 170 (2008). Crossref
6. E. Shel. SPE Russian Petroleum Technology Conference, Moscow, Russia, SPE-187834-MS (2017). Crossref
7. A. M. Linkov. J. Appl. Math. Mech. 79 (1), 54 (2015). Crossref
8. A. M. Linkov. Dokl. Phys. 61 (7), 350 (2016). Crossref
9. A. M. Linkov. Boundary integral equations in elasticity theory. Springer Science and Business Media (2013) 99 p. Crossref
10. A. M. Linkov, A. A. Linkova, A. A. Savitski. Int. J. Dam. Mech. 3 (4), 338 (1994). Crossref
11. N. S. Markov, A. M. Linkov. Mater. Phys. Mech. 32 (2), 133 (2017). Crossref
12. G. S. Mishuris. Mech. Compos. Mater. 34, 439 (1998). Crossref
13. A. M. Krivtsov. Deformation and fracture of solids with microstructure. Moscow, Fizmatlit (2007) 304 p. (in Russian)
14. B. Damjanac, P. Cundal. Comput. Geotech. 71, 283 (2016). Crossref
15. A. M. Krivtsov. Int. J. Imp. Eng. 23, 477 (1999). Crossref
16. A. M. Krivtsov. Meccanica. 38 (1), 61 (2003). Crossref
17. D. A. Indeitsev, A. M. Krivtsov, P. V. Tkachev. Dokl. Phys. 51 (3), 154 (2006). Crossref
18. V. A. Tsaplin, V. A. Kuzkin. Mater. Phys. Mech. 32 (3), 321 (2017).
19. R. A. Jarvis. Inf. Process. Lett. 2, 18 (1973). Crossref
20. P. Livieri, F. Segala. Eng. Fract. Mech. 77 (11), 1656 (2010). Crossref
21. V. Lazarus. J. Mech. Phys. Sol. 59, 121 (2011). Crossref
22. R. V. Goldstein, V. M. Entov. Qualitative Methods in Continuum Mechanics. Nauka, Moscow (1989) 224 p. (in Russian)